HHS Public Access

Author manuscript

Oncogene. Author manuscript; available in PMC 2016 February 20.

Published in final edited form as:

Oncogene. 2015 August 20; 34(34): 4519–4530. doi:10.1038/onc.2014.386.

Role of bacterial infection in the epigenetic regulation of Wnt antagonist WIF1 by PRC2 protein EZH2

Badal C. Roy[1], **Dharmalingam Subramaniam**[1], **Ishfaq Ahmed**[1], **Venkatakrishna R. Jala**[3], **Christina Hester**[1], **K. Allen Greiner**[1], **Bodduluri Haribabu**[3], **Shrikant Anant**[1,4], and **Shahid Umar**[1,4,*]

[1]Departments of Molecular and Integrative Physiology and Family Medicine Research Division, University of Kansas Medical Center, Kansas City, KS, 66160

[2]Department of Diagnostic Medicine/Pathobiology, College of Veterinary Medicine, Kansas State University, Manhattan, KS 66506

[3]James Graham Brown Cancer Center and Department of Microbiology and Immunology, University of Louisville, Louisville, KY 40202

[4]University of Kansas Cancer Center, Kansas City, KS, 66160

Abstract

The Enhancer of Zeste Homolog-2 (EZH2) represses gene transcription through histone H3 lysine-27-trimethylation (H3K27me3). *Citrobacter rodentium* (CR) promotes crypt hyperplasia and tumorigenesis by aberrantly regulating Wnt/β-catenin signaling. We aimed at investigating EZH2's role in epigenetically regulating Wnt/β-catenin signaling following bacterial infection. NIH:Swiss outbred and $Apc^{Min/+}$ mice were infected with CR (10^8cfu); $BLT1^{-/-}Apc^{Min/+}$ mice, AOM/DSS-treated mice and de-identified human adenocarcinoma samples were models of colon cancer. Following infection with wild type but not mutant CR, elevated EZH2 levels in the crypt at days-6 and 12 (peak hyperplasia) coincided with increases in H3K27me3 and β-catenin levels, respectively. Chromatin immunoprecipitation revealed EZH2 and H3K27me3's occupancy on WIF1 (Wnt Inhibitory Factor-1) promoter resulting in reduced WIF1 mRNA and protein expression. Following EZH2 knockdown via siRNA or EZH2-inhibitor DZNep either alone or in combination with HDAC inhibitor SAHA, WIF1 promoter activity increased significantly while overexpression of EZH2 attenuated WIF1-reporter activity. Ectopic overexpression of SET domain mutant (F681Y) almost completely rescued WIF1 reporter activity and partially rescued WIF1 protein levels while H3K27me3 levels were significantly attenuated suggesting that an intact methyltransferases activity is required for EZH2-dependent effects. Interestingly, while β-catenin levels were lower in EZH2-knocked-down cells, F681Y mutants exhibited only partial reduction in β-catenin levels. Besides EZH2, increases in miR-203 expression in the crypts at days-6 and 12 post-infection correlated with reduced levels of its target WIF1; overexpression of

Address for Correspondence: Shahid Umar, PhD, Associate Professor, Member – University of Kansas Cancer Center, University of Kansas Medical Center, 3901 Rainbow Blvd, 4028 Wahl Hall East, Kansas City, KS, 66160 Phone: (913) - 945-6337 Fax: (913) - 945-6327, sumar@kumc.edu.

Disclosures- The authors disclose no conflicts.

miR-203 in primary colonocytes decreased WIF1 mRNA and protein levels. Elevated levels of EZH2 and β-catenin with concomitant decrease in WIF1 expression in the polyps of CR-infected *Apc*$^{Min/+}$ mice paralleled changes recorded in *BLT1*$^{-/-}$*Apc*$^{Min/+}$, AOM/DSS and human adenocarcinomas. Thus, EZH2-induced downregulation of WIF1 expression may partially regulate Wnt/β-catenin-dependent crypt hyperplasia in response to CR infection.

Keywords

Bacterial infection; Epigenetics; EZH2; Wnt-antagonist WIF1; Hyperplasia; Colon Cancer

Introduction

Enhancer of Zeste Homolog-2 (EZH2) is the catalytic component of PRC2 that catalyzes trimethylation of its substrate H3K27 which is usually associated with transcriptional silencing. Adult tissues generally lack EZH2 expression. However, higher proliferative index is commonly associated with EZH2 overexpression in cancer. Indeed, loss of EZH2 inhibits growth of cancer cells, induces senescence and apoptosis and decreases invasion and metastasis [20, 24, 26]. EZH2 overexpression and tumor invasiveness or metastasis has been corroborated by the suppressing function of EZH2 on the expression of several miRNAs that regulate PRC1, KLF2, EMT-suppressor E-cadherin [5, 6, 31, 38] while EZH2 itself is regulated by miRNAs like miR-26a and miR-101[23].

Wnt/β-catenin signaling plays important roles during normal cellular development. Aberrant activation of Wnt/β-catenin is associated with various human diseases including cancer [12]. Loss-of-function mutations in *Apc* gene (encoding APC) and gain-of-function mutation in *CTNNB1* (encoding β-catenin) have been suggested as the chronic preferred route of Wnt-signaling deregulation in cancer. But abnormal accumulation of β-catenin does not always correlate with mutational activation as was evident in hepatocellular carcinoma [7] suggesting that epigenetic mechanism may work in tandem with genetic changes to modulate the process of Wnt/β-catenin-induced cellular transformation and tumorigenesis.

Citrobacter rodentium-induced transmissible murine colonic hyperplasia (TMCH) that utilizes a type three secretion system (T3SS) to activate Wnt/β-catenin signaling represents the earliest molecular and functional changes associated with colon carcinogenesis. Employing this model, we showed previously that increases in β-catenin that correlates with colonic crypt hyperplasia, are neither due to mutations in *Apc* or *CTNNB1* gene, respectively[1, 10, 28, 32-34]. More recently, we showed that distinct changes in expression of HDACs, Histone methyltransferases SMYD3 and EZH2 and in their substrates H3K4me3 and H3K27me3 respectively, were associated with crypt hyperplasia and EMT (Epithelial-Mesenchymal Transition) [10]. EZH2 also interacts with HDACs in transcriptional silencing to promote loss of tumor suppressor function while overexpression of EZH2 is a marker of advanced and metastatic disease in many solid tumors, including colon cancer. Yet, how EZH2 regulates β-catenin-dependent Wnt signaling within the colonic crypts and whether EZH2/β-catenin-mediated downregulation of Wnt antagonists [e.g., Wnt Inhibitory Factor 1 (WIF1)] plays a role in CR-induced crypt hyperplasia and tumorigenesis, is not known.

Similarly, microRNAs (miRNAs) are short (~22 bp length) noncoding RNAs that regulate gene expression post-transcriptionally by binding to the 3'UTR-region of the target genes thereby either destabilizing mRNA or inhibiting translation. Yet, how miRNAs are involved in regulating the components of Wnt signaling *in vivo* is less understood. We therefore hypothesized that CR infection-induced epigenetic remodeling may underlie Wnt/β-catenin-dependent crypt hyperplasia and tumorigenesis. This hypothesis was tested in the current study.

Results

Effect of CR infection on the expression of PcG protein EZH2

In a recent study, we showed significant alterations in the expression of HDACs, histone methyltransferases SMYD3 and EZH2 and in their substrates H3K4me3 and H3K27me3, respectively, in the colonic crypts in response to CR infection [10]. Modulation of host transcription by pathogens is well accepted; yet, how specific epigenetic programs are controlled by pathogens is not known. EZH2 is overexpressed in several malignancies including colon cancer; EZH2's role in tumor initiation however, is less clear. During immuno-staining with anti-EZH2, distal colonic sections from uninfected control mice exhibited nuclear staining predominantly at the base of the crypt. At day 6 and particularly at day 12, intense nuclear staining extending throughout the longitudinal crypt axis was recorded (**Fig. 1A**). At days 20, 27 and 34, a downward trend of EZH2 immunoreactivity was observed (**Fig. 1A**). To determine whether these changes are specifically induced by CR or they are normal host responses to CR infection, we infected NIH:Swiss outbred mice with wild type CR or ΔescV T3SS mutant which fails to inject CR's effector proteins into the host [13]. In response to wild type CR, we observed a predictable crypt hyperplasia at 12 days' post infection as was evident following PCNA staining while no such increase was recorded with ΔescV (**Fig. 1B**). Interestingly, EZH2 exhibited dramatic co-localization with PCNA in response to wild type CR at day 12 while the extent of co-localization with ΔescV paralleled that of uninfected control (**Fig. 1B**). Western blot analyses showed wild type CR-induced increases in EZH2, H3K27me3, β-catenin, SMYD3 and HDAC1 while ΔescV mutant exhibited an attenuated response (**Fig. 1C**). Thus, increases in crypt EZH2, H3K27me3, β-catenin etc., are specific to infection by wild type CR and correlate with levels recorded during advanced carcinomas [3, 19]. For functional assays *in vitro*, we chose human embryonic kidney HEK293-T cells that offer better transfection efficiency. In HEK-293T cells, CR infection induced significant increases in EZH2's mRNA expression (**Supplementary Fig. 1Ai**). Knockdown of EZH2 confirmed either at the mRNA or protein level (**Supplementary Fig. 1Aii, B**) was associated with significant decrease in β-catenin abundance suggesting EZH2's involvement in Wnt signaling. Next we performed wound healing and spheroid assays to determine if EZH2 was functionally relevant. Following knockdown of EZH2 via specific siRNA, cell migration was significantly inhibited when compared to cells treated with control siRNA (**Supplementary Fig. 1C**). This is consistent with EZH2's role as a promoter of metastasis and malignancy [27]. Recent studies have also implicated EZH2 in the maintenance of stem cells [27]. Since the ability to self-renew is a hallmark of stem cells and the formation of epithelial-like colonies (spheroids) is an index of self-renewal [36], we performed spheroid assay in either HEK-293T or HCT116 cells, respectively. EZH2

depletion dramatically reduced the size and number of spheroids in either cell line (**Supplementary Fig. 1D**) indicating that EZH2 is required for stem cell maintenance. Indeed, real-time PCR for cancer stem cell (CSC) markers revealed significant reduction in CD44 and Dclk1expression following EZH2 knockdown while expression of Lgr5 was less affected in HEK-293 cells (**Supplementary Figs. 1E-G**). Interestingly, EZH2 knockdown in HCT116 cells had more pronounced effect on downregulation of these CSC markers (**Supplementary Fig. 2**). Thus, EZH2 is efficiently induced in the colonic crypts in response to bacterial infection wherein, it mimics conditions reminiscent of advanced stages of colon cancer despite CR infection being a self-limiting disease.

Novel regulation of Wnt antagonist WIF1 by EZH2

We showed recently that EZH2 depletion led to significant decrease in β-catenin/Tcf4-dependent TOP-Flash reporter activity due to loss of β-catenin [10]. This finding prompted us to speculate that EZH2 depletion may lead to de-repression of Wnt antagonists thereby attenuating Wnt signaling. To examine this, we knocked down EZH2 with specific siRNA and analyzed the expression levels of Wnt antagonists Dkk1, Dkk2, Dkk3, sFRP1, sFRP2, sFRP4 and WIF1 via real-time RT-PCR. Among these genes, only WIF1 transcript exhibited any significant upregulation following EZH2 knockdown (**Figure 2A-Ci**). This was also confirmed at the protein level by Western blotting the total extracts (**Supplementary Fig. 3A)**. These changes in expression of Wnt antagonists were also compared with ΔescV mutant and as depicted in **Supplementary Figs. 3Bi-Ciii**, except for sFRP2, the expression levels returned to baseline with mutant CR. To replicate these changes in primary cells, we utilized immortalized young adult mouse colon (YAMC) cells wherein, CR infection induced significant increases in EZH2 expression both at 24 and 72 hr while WIF1 expression was likewise downregulated at these time points (**Supplementary Figs. 3Di, Dii**). Interestingly, infection with CR mutant ΔescV attenuated either increase in EZH2 or decrease in WIF1 expression (**Supplementary Figs. 3Ei, Eii**). Finally, overexpression of EZH2 in YAMC cells, confirmed at the mRNA level (**Supplementary Fig. 3Fi**) was associated with significant decrease in WIF1 expression (**Supplementary Fig. 3Fii**). Next we performed WIF1 expression analysis in the isolated crypts. As depicted in **Fig. 2Cii**, WIF1 expression was high in uninfected crypts. At days 6 and 12, significant attenuation of WIF1 expression was recorded. Interestingly, WIF1 expression returned to baseline at day 34 (**Fig. 2Cii**) consistent with regressing phase of crypt hyperplasia [8]. During immunohistochemistry, we observed dramatic decreases in crypt WIF1 immunoreactivity at days 6-20 compared to uninfected control (**Figure 2D**). At days 27 and 34, we observed significant rebound in WIF1 staining in the crypt regions while stromal staining was consistent with WIF1 being a secretory protein (**Figure 2D**). **Figure 2E** is the line plot demonstrating reciprocal relationship between EZH2 and WIF1. This reciprocal relationship between EZH2 and WIF1 was further validated in a series of distal colonic sections from wither NIH:Swiss outbred mice or $Apc^{Min/+}$ mice wherein, co-localization studies revealed EZH2 staining in only those areas that were negative for WIF1 and vice-versa (**Supplementary Fig. 4**). Thus, a reciprocal relationship between EZH2 and WIF1 wherein, high EZH2 levels (mRNA or protein) coincident with progression of hyperplasia preceded elevated accumulation of WIF1 when the crypt hyperplasia was regressing [8].

Transcriptional repression of WIF1 by EZH2's recruitment to *WIF1* promoter

Next, we set out to understand whether the reciprocal relationship between EZH2 and WIF1 could be a result of a direct effect of EZH2 on the WIF1 promoter. We performed quantitative chromatin immunoprecipitation (qChIP) in day 6 crypt DNA samples for the minimal promoter of WIF1 using antibodies against EZH2 and H3K27me3 proteins, respectively. **Supplementary Fig. 5** depicts the sequence of the mouse WIF1 promoter. A 1.66 kb fragment amplified using mouse genomic DNA as a template was sequenced with primers shown in boxes. The sequence was obtained from the mouse genome sequence database at the UCSF web server (http://genome.ucsf.edu) using the promoter search program (http://gpminer.mbc.nctu.edu.tw). **Figure 3A** represents the regions in the mouse WIF1 promoter, located at chromosome position 10, that were analyzed via qChIP. As depicted in **Figure 3Bi and Bii**, the qChIP analyses exhibited an enriched presence of EZH2 and H3K27me3 on the WIF1 promoter relative to uninfected control. Intriguingly, the promoter region with maximum binding to EZH2 was observed to be distal to the region where maximum H3K27me3 modification occurred suggesting that EZH2's role in either WIF1 downregulation or β-catenin upregulation, may be independent of its methyltransferase activity. This is not unprecedented since Jung HY et al.[18] recently demonstrated that PAF (PCNA-associated factor) recruits EZH2 to the β-catenin transcriptional complex and specifically enhances Wnt signaling independently of EZH2's methyltransferase activity. To begin to unravel the mystery of EZH2 and H3K27me3's regulation of WIF1 promoter, we adopted two different strategies. First, we cloned a 1.66 kb regulatory region of mouse *WIF1* containing the EZH2-binding regions (**Fig. 3A**) to a pGL3 luciferase reporter construct for promoter assay. During measurement of mouse WIF1 promoter activity in HEK-293T cells, knockdown of EZH2 with specific siRNAs significantly increased WIF1 reporter activity (**Fig. 3Ci**). Since histone deacetylase (HDAC) activity is associated with transcriptional repression [19, 38] and based on significant upregulation of HDACs in the colonic crypts in response to CR infection [10], we next examined if HDACs could be part of the repressive complex that catalyzed the transcriptional repression of WIF1. Indeed, treatment with HDAC inhibitor SAHA either alone or in combination with DZNep reversed EZH2-mediated repression of the WIF1 promoter activity (**Fig. 3Cii**), indicating that HDAC activity is complementary to EZH2-mediated WIF1 suppression. Secondly, we mutated the tyrosine-681 in the catalytic domain of EZH2 that regulates its enzymatic activity [17]. Ectopic overexpression of F681Y mutant almost completely rescued WIF1 reporter activity and partially rescued WIF1 protein levels while H3K27me3 levels were completely attenuated (**Fig. 3Di, Dii**) suggesting that an intact methyltransferase activity is required for EZH2-dependent effects. Interestingly, while β-catenin levels were lower in EZH2-knocked-down cells, F681Y mutant exhibited only partial reduction in β-catenin levels (**Fig. 3Di, Dii**). To establish a direct role for WIF1 in downregulating Wnt signaling, we overexpressed both EZH2 and WIF1 in HEK-293 cells and measured TopFlash reporter activity. As depicted in **Figure 3E**, EZH2 overexpression significantly increased the TopFlash activity as expected while overexpression of WIF1 resulted in almost complete attenuation of TopFlash activity suggesting antagonism of WIF1-induced Wnt signaling.

Next in a series of experiments to further validate the reciprocal relationship between EZH2 and WIF1, we performed reporter assays with human promoter for WIF1 to see if EZH2 is also involved in WIF1 repression in humans. Knockdown of EZH2 significantly increased while overexpression of EZH2 resulted in decrease in WIF1-reporter activity (**Supplementary Fig. 6A, B**). Both DZNeP and SAHA either alone or in combination reversed the inhibitory effects (**Supplementary Fig. 6C**). In addition, we utilized another known HDAC inhibitor, sodium butyrate (NaB) [4] to further assess the effect of HDAC inhibition on WIF1 mRNA. As expected, NaB significantly blocked CR-induced increases in EZH2 and H3K27me3 both at the mRNA and protein level (**Supplementary Figs. 6D, E**) while concomitantly increasing WIF1 mRNA levels 10 fold (**Supplementary Fig. 6F**). Finally, during WIF1 reporter assay in HCT116 human colon cancer cell line, knockdown of EZH2 likewise increased the WIF1 reporter activity while treatment with DZNeP or SAHA either alone or in combination yielded results (**Supplementary Figs. 6G, H**) similar to those recorded in HEK-293T cells. Collectively, these data suggest that EZH2 in cooperation with HDACs, transcriptionally repress WIF1 probably via histone methylation and deacetylation.

MicroRNA regulation of WIF1 transcription

Since miRNAs are component of epigenetic regulation, we set out to assess the contribution of miRNAs in mouse colonic hyperplasia. Total crypt RNA isolated from uninfected normal or days 6-34 post-CR infected distal colons was subjected to a miRNA array. As depicted in **Figure 4A**, a heat map was generated showing the differential expression intensities of indicated miRNAs. Among the most upregulated ones, miR-7a, miR-17, miR-20a, miR-21, miR-142-3p and miR-203 were further validated via real-time RT-PCR (**Figure 4Bi-Bvi**). Of these miRNAs, we were particularly interested in miR-203 due to its involvement in Wnt signaling and EMT [36]. To identify the targets of miR-203, we used miRNA target analysis (www.targetscan.org) and found a number of putative target genes such as *Dkk1*, *Nkd1*, *WIF1*, *sFRP1*, *APC*, *KL4*, *NLK and TCF4* that are associated with Wnt signaling. We selected WIF1 as one of the targets of miR-203 for several reasons. We wanted to explore whether: (a) CR-induced changes in either miR-203 or EZH2 mimic what happens during the late stages of colon carcinogenesis and, (b) whether WIF1 that exhibited the greatest change in its expression following EZH2 knockdown (see **Fig. 2Ci**), could be the bridging molecule to link both miR-203 and EZH2 to Wnt signaling. The predicted binding site of miR-203 in the 3'-UTR sequence of *WIF1* (**Figure 4C**) was cloned downstream of the firefly luciferase gene in the pGL4-NF-κB-Luc vector. When the cells were co-transfected with miR-203 and pGL4-NF-κB-Luc 3'UTR-WT, there was a significant reduction in luciferase activity compared with cells transfected with the control vector (**Figure 4Di**). In addition, HEK-293T cells stably expressing miR-203 when co-transfected with the above construct exhibited significant decrease in luciferase activity while overexpression of miR-21 had no effect on reporter activity (**Figure 4Dii**). To further validate miR-203's dependence on 3'-UTR to block WIF1 function, we mutated the 3'-UTR site and following transfection into HEK-293T cells, compared the reporter activity with wild type counterpart. Indeed, cells expressing wild type 3'-UTR exhibited significant decrease in reporter activity in response to miR-203 overexpression whereas a construct, pGL4-NF-κB-Luc-3'UTR-*mut*, expressing mutated 3'-UTR failed to exhibit any change in the luciferase activity (**Figure 4Diii**). Finally in a two-pronged approach, overexpression of miR-203 but not miR-21 or

miR-142-3p reduced the WIF1 mRNA (**Fig 4E**) as well as protein levels (**Fig. 4F**), respectively. Thus, we provide evidence for epigenetic regulation of Wnt antagonist WIF1 by EZH2 and miR-203.

EZH2 expression negatively correlates with WIF1 levels and positively with β-catenin accumulation in mouse and human adenoma/adenocarcinoma

To validate the inverse association between EZH2 and WIF1, we examined the staining intensities of EZH2 and WIF1 in four different models of colon cancer. We [2, 9] and others [25] have shown that $Apc^{Min/+}$ mice when infected with CR exhibit exaggerated tumorigenesis in the distal colon, the site of CR infection. As depicted in **Figure 5A**, EZH2 staining in the uninfected control mice was mostly restricted to the basal 1/3rd of the crypt. Following CR infection, the entire adenoma developed in the distal colon at 12 weeks exhibited intense EZH2 staining that correlated with similar increases in β-catenin staining compared to uninfected control (**Figure 5A**). WIF1 staining on the other hand, was significantly higher in the uninfected control while a dramatic loss of WIF1 staining was associated with CR-induced increases in colonic tumors in these mice (**Figure 5A**). These changes are usually associated with adenocarcinomas in humans and poor prognosis [3, 19] suggesting that CR infection mimics human conditions despite being a self-limiting disease.

Leukotriene B4 (LTB4)-induced signaling pathway that mediates its actions via high affinity G protein-coupled receptor BLT1, is implicated in human colon cancer [16]. We have developed a novel model of spontaneous intestinal cancer by crossing the $BLT1^{-/-}$ mice with $Apc^{Min/+}$ mice wherein, $BLT1^{-/-}Apc^{Min/+}$ mice exhibit an exaggerated tumorigenesis in the intestine and particularly in the colon compared to $BLT1^{-/-}$ mice alone (manuscript in preparation). Using $BLT1^{-/-}Apc^{Min/+}$ mice as a model of spontaneous colon tumorigenesis, we observed no detectable EZH2 staining in $BLT1^{-/-}$ control mice while a dramatic increase in EZH2 staining encompassing the entire adenoma was recorded in the $BLT1^{-/-}Apc^{Min/+}$ mice at 110 days that correlated positively with increases in β-catenin nuclear staining (**Figure 5B**) and coincided with dramatic decrease in WIF1 staining compared to $BLT1^{-/-}$ mice alone (**Figure 5B**). These findings were further validated in a murine model of colitis-associated colon cancer wherein, adenoma was initiated with azoxymethane (AOM) treatment followed by dextran sodium sulfate (DSS) ingestion in ICR outbred mice. As depicted in **Figure 5C**, increases in EZH2 and its substrate, H3K27me3 and β-catenin immunostaining in the distal colons of AOM/DSS-treated mice coincided with dramatic loss of WIF1 staining compared to either untreated (**Figure 5C**) or AOM or DSS-treated mice (data not shown), respectively. During analysis of human adenocarcinoma or adenocarcinoma with an invasive front, adjacent mucosa exhibited EZH2 nuclear staining mostly at the base of the crypt (**Figure 6A**). In adenocarcinomas, the entire longitudinal crypt axis as well as the invasive front exhibited intense nuclear staining for EZH2 (**Figure 6A**). Similarly, we observed mostly membranous staining for β-catenin in the adjacent mucosa while staining was intense and predominantly nuclear in the adenocarcinomas (**Figure 6A**). In contrast, WIF1 staining, while intense in the adjacent mucosa, was almost non-detectable in the areas of adenocarcinomas that were positive for EZH2 (**Figure 6B**).

Discussion

Bacterial pathogens promote histone modifications and chromatin remodeling as an important strategy to interfere with key cellular processes in the infected cells [14]. We recently showed that CR infection induced significant alterations in epigenetic signaling in the distal colon that coincided with Wnt/β-catenin, Notch and NF-κB-dependent increases in colonic crypt hyperplasia [1, 10, 28, 29, 32-34]. In the current study, we describe a novel mechanism by which Wnt antagonist WIF1 is downregulated in EZH2-overexpressing cells through histone H3K27 trimethylation at the WIF1 promoter which may be directly involved in epigenetic upregulation of β-catenin function in response to CR infection. While these findings are consistent with either targeted overexpression of EZH2 in the mammary gland that causes epithelial hyperplasia [21] or in response to *H. pylori* CagA-mediated aberrant epigenetic silencing that induces Ras upregulation [15], CR-induced EZH2 upregulation in a non-transformed colonic epithelium mimics advanced stages of colon carcinogenesis despite TMCH being a self-limiting disease [35]. We have further discovered that blocking EZH2 function *in vitro* inhibited cell migration and spheroid growth due to decreases in CSC markers CD44, Dclk1 and Lgr5. This is consistent with EZH2's role in self-renewal, pluripotency and proliferation of cancer stem cells [30]. Interestingly, elevated EZH2 expression resulted in increased accumulation of EZH2 itself along with its target H3K27me3 on the *WIF1* promoter which led to significant downregulation of WIF1 expression (see **Figure 3**). Wnt antagonists are natural inhibitors of Wnt/β-catenin signaling that work in different subcellular compartments in the cell. Epigenetic silencing of these inhibitors allows constitutive Wnt/β-catenin signaling in various cancers [7, 11]. Inactivation of Wnt antagonist WIF1, mostly through DNA hypermethylation of the promoter region has been reported as an early event in various cancers even though fewer studies suggest a correlation between loss of WIF1 expression and disease progression [37]. On the other hand, a recent study by Kondo et al., [20] suggested that gene silencing by histone H3K27 trimethylation was independent of the WIF1 promoter methylation. Our findings support this notion that EZH2 and its target, H3K27me3's accumulation on the WIF1 promoter, at least in part, silences its expression. Intriguingly, ChIP assays also revealed discrepancy between EZH2 and H3K27me3 amplicons suggesting the notion that EZH2's regulation of Wnt/β-catenin signaling may be uncoupled with its methyltransferase function. Studies with catalytic domain mutant F681Y of EZH2 [17] revealed significant recovery of WIF1 reporter activity while H3K27me3 levels were completely attenuated which to some extent, ruled out the possibility that EZH2's methyltransferase function is irrelevant to its epigenetic regulation of WIF1 expression. Whether WIF1 demethylation is responsible for this reversal in WIF1 function following point mutation in EZH2 however, remains to be delineated. Interestingly, F681Y mutant exhibited only partial reduction in β-catenin levels suggesting that point mutations in EZH2 may not be sufficient by themselves to block Wnt signaling and that residual endogenous EZH2 may be enough to promote Wnt/β-catenin signaling. Nonetheless, a direct role for WIF1 in downregulating Wnt signaling was revealed by WIF1 overexpression that resulted in almost complete attenuation of TopFlash activity. It is also worth mentioning that EZH2 also interacts with HDACs in transcriptional silencing to promote loss of tumor suppressor function. Indeed, HDACs seem to be an important component of the EZH2-mediated WIF1 repression in our model, as cells treated with

HDAC inhibitor sodium butyrate (NaB) reversed the suppressive activity of EZH2 on the WIF1 promoter suggesting that EZH2 catalytic activity or EZH2-mediated H3K27me3 accumulation on the WIF1 promoter alone may not be sufficient for promoter silencing; rather repressing enzymes including HDACs may be necessary for further chromatin condensation and transcriptional repression. This is consistent with our previous report wherein, HDAC1-4 upregulation observed during CR-induced colonic crypt hyperplasia [10] may corroborate with EZH2 to promote epigenetic silencing of WIF1 [19] thereby atleast partially regulating Wnt/β-catenin signaling.

We also delineated another mechanism of WIF1 transcriptional regulation by miRNA. Following a microarray analysis, miR-203 along with several other miRNAs, was upregulated several fold in the colonic crypts of CR infected mice (see **Fig. 4**). Data base search of miR-203 revealed several putative target genes related to Wnt/β-catenin signaling pathway including WIF1. In the current study, we provide evidence that WIF1 was regulated by miR-203 suggesting that miR-203 may corroborate with EZH2 to repress WIF1 expression in response to CR infection. This is consistent with a recent report wherein, CagA was shown to induce aberrant epigenetic silencing of let-7 expression leading to Ras upregulation during *H. pylori*-related gastric carcinogenesis [15] suggesting that infection-induced deregulation of epigenetics and miRNA expression may be a novel potential target for the prevention of gastric or colon carcinogenesis, respectively.

We have employed an animal model (TMCH) that involves the earliest molecular and functional changes associated with colon carcinogenesis. However, if TMCH is a unique response to a peculiar bacterium, it may not be of general interest. To rule out this possibility, we examined mice that either develop spontaneous colon cancer ($BLT1^{-/-}Apc^{Min/+}$) as well as mice that developed colon cancer in response to mutagenic and inflammatory insults. Finally, we also capitalized on the availability of human adenocarcinomas from our biospecimen repository to establish relevance of our studies to humans. During a thorough and systematic analysis, we discovered that changes recorded in EZH2 and β-catenin expression in the distal colons of either $BLT1^{-/-}Apc^{Min/+}$ mice or AOM/DSS-treated mice were mirror images of those recorded during CR infection. Similarly, human adenocarcinomas with and without invasive front, exhibited aberrant EZH2 and β-catenin nuclear staining that paralleled changes recorded during CR infection. The increases in EZH2 and β-catenin staining in either murine or human tissues were associated with concomitant decreases in WIF1 staining suggesting a tumor suppressing function of WIF1 that may have been epigenetically repressed to promote Wnt signaling. These findings are consistent with EZH2's role in silencing several anti-metastatic genes (e.g., E-cadherin) to promote cell invasion and anchorage-independent growth [22]. Thus, the epigenetic signaling pattern in the CR model is not unique but shares a common final pathway with seemingly diverse models of colonic crypt proliferation and carcinogenesis and that the findings in the CR model may very well have broader pathophysiologic and clinical significance.

Materials and Methods

Mice, *Citrobacter rodentium* infection, murine and human models of colon cancer

This study was carried out in strict accordance with the recommendations in the Guide for the Care and Use of Laboratory Animals of the National Institutes of Health. All protocols were approved by University of Kansas Medical Center Animal Care and Use Committee. All efforts were made to minimize suffering. Male *Helicobacter pylori*-free NIH:Swiss and $Apc^{Min/+}$ mice were procured from Jackson Laboratory, Bar Harbor, Maine, USA. NIH:Swiss or $Apc^{Min/+}$ mice were infected by oral inoculation with a 16-h culture of CR (biotype 4280, ATCC, 10^8CFUs) identified as pink colonies on MacConkey agar, as previously described [1]. Age- and sex-matched control mice received sterile culture medium only. $BLT1^{-/-}$ and $BLT1^{-/-}Apc^{Min/+}$ mice were developed in the laboratory of Dr. Bodduluri Haribabu, Professor, University of Louisville, and bred at KU Medical Center. For AOM/DSS model following intraperitoneal pretreatment with azoxymethane (10mg/kg b.w.), the animals were subjected to three cycles of alternating administration of 2.5% DSS for seven days followed by distilled water for the subsequent 14 days. Mice were euthanized at 24 weeks. Colonic crypts were isolated as described [1, 2, 8, 10, 28, 29, 32-34]. De-identified and paraffin-embedded human adenocarcinoma sections were kindly provided by University of Kansas Cancer Center Biospecimen Repository Core.

Cell Lines and Plasmids

Unless mentioned otherwise, all cell lines were obtained from American Type Culture Collection (Rockville, MD). All cells were grown in 5% CO_2, DMEM or RPMI containing10% fetal bovine serum and penicillin/streptomycin. YAMC were cultured as described elsewhere [10]. All plasmid constructs sequences were verified by automated DNA sequencing. Drug selection on pEZX-miRNAs (GeneCopoeia, Rockville, MD) transduced cells was carried out in puromycin (1.0 μg/ml) (Sigma). Control, containing a scrambled sequences, transduction was carried out in parallel. All the transduced cells were subsequently cultured in media containing 1.0 μg/ml puromycin (Sigma).

Western Blot Analysis

Total crypt cellular or nuclear extracts were prepared as described [1]. Cell lysates, from cell lines, were prepared in RIPA (radioimmunoprecipitation assay) buffer with complete protease inhibitors (Roche Applied Science, IN, USA). Western blots were performed as described before [2] .

RNA isolation and quantitative RT–PCR

Total RNA was isolated from crypts or crypt-denuded lamina propria (CLP) from the distal colons of uninfected or CR-infected mice at selected time points using TRIzol™ reagent. Expression levels of mRNA in the colonic crypts or CLP were measured by synthesis of cDNA from 2ug of total RNA a high capacity cDNA reverse transcription kit (Applied Biosystems, Foster City, CA, USA). cDNAs were used for real-time PCR using Jumpstart *Taq* DNA polymerase (Sigma-Aldrich) and SYBR Green (Molecular Probes, Eugene, OR) nucleic acid stain as a marker for DNA amplification on a Bio-Rad CFX96 Touch™ Real-

Time PCR Detection System. Relative fold change values were calculated with the comparative threshold cycle (ΔCt) method normalized to GAPDH. Changes in mRNA expression were expressed as fold change relative to control. Primer sequences for all target genes and internal control are shown in Supplementary Table S1.

Chromatin Immunoprecipitation (ChIP)

ChIP Assays were performed as described [10]. We used the following antibodies in the ChIP study: anti-EZH2, anti-H3K27me3 (Cell Signaling). All the experiments in tissue specimens were repeated at least three times. The sequences of the PCR primers are shown in Supplementary Table S2.

Reporter Gene Assays

Reporter activities were measured as described [10]. Briefly, at 24 h post transfection, cells were infected with CR at multiplicity of infection (MOI) of 90 for 3 h. Cells were then washed to remove the bacteria and incubated at 37°C with or without drugs for 24 and 48 h. Synergy H4 hybrid microplate reader (Bio Trek) was used to measure the luminescence.

Construction of the human and mouse WIF-1 promoter regions and measurement of promoter reporter activities

Reporter vector containing regions of Human *WIF1* (−1463 to −102) promoter (HPRM16566-PG02; GeneCopoeia) was sub cloned in pGL3-Luc basic vector (Promega). For cloning of mouse WIF1 promoter, we used a PCR-based technique. Sense (5'-TGTCTAACTCCCAAACACAATACC-3') and anti-sense (5'-TCCGAGCCATGGTGCTCAGGACC-3') primers were chosen from the genomic sequence of the mouse WIF-1 gene (Accession No. AC153357), corresponding to the sequence −1653 to +10 (the start codon ATG of mouse WIF-1 gene is defined as +1). PrimeSTAR GXL PCR (Clontech, Mountain View, CA) (30 cycles) was performed. All the sequences were verified by DNA sequencing (ACGT, Inc., Wheeling, IL). Cells were co-transfected using 1.0 μg of each DNA construct in pGL3Basic vector and 0.05 μg of pRL-TK Vector (Promega, Madison, WI) containing Renilla luciferase as an internal control for the transfection efficiency. For co-transfection, siEZH2 or EZH2 expression vectors were transfected simultaneously along with reporter constructs. Lipofectamine 2000 (Invitrogen, Carlsbad, CA) was used. Reporter activity was measured as above. HEK-293T cells were treated with 1μM suberoylanilide hydroxamic acid (SAHA), 2.5 mM of NaB and 2.5 μM deazaneplanocin A (DZNep) or in combination for 40 hrs followed by Luciferase reporter assay.

miRNAs Assay and 3'-UTR cloning

All miRNAs assay kits were purchased from ABI (Life Technologies). Small nuclear RNA U6 were used as an internal control and relative fold change values were calculated with the comparative threshold cycle (ΔCt) method normalized to U6. The luciferase reporter gene construct containing the miR-203 targeting site from the 3′-UTR of *WIF1* or others was created by cloning around 40-bp fragment (positions 1890 to 1930, NM_007191), containing the miRNA-203 binding site into the EcoI site on the 3′-region of the luciferase

gene in the pGL4.32 (Luc2P/NF-κB197 RE/hygro) firefly luciferase reporter vector (Promega). A mutant construct of the above was made the same way. The constructs were sequenced to check the proper orientation or to eliminate any undesired mutation. 293T cells were transfected with either the construct above or [pGL4.15 [*luc2p*/Hygro] vector as control (from Promega), using Lipofectamine 2000 transfection reagent (Invitrogen). After 24h of transfection, luciferase activity was measured using a Bright Glo Luciferase assay system (Promega,Madison,WI).

Histology and immunohistochemistry

For histology, tissues were fixed in 10% neutral buffered formalin or Carnoy's fixative (60% methanol, 30% chloroform, and 10% acetic acid) prior to paraffin embedding. Images were obtained with an Eclipse E1000 microscope (Nikon). Immunohistochemistry (IHC) to detect EZH2, H3K27me3, (antibodies from Cell Signaling), β-catenin (BD, Transduction) and WIF1 (Abcam) was performed on 5-μm-thick paraffin-embedded sections prepared from the distal colons of groups of mice described elsewhere utilizing the horseradish peroxidase (HRP)-labeled polymer conjugated to secondary antibody using the Histostain-SP Kit (DAB, Broad Spectrum) (Invitrogen) with microwave accentuation, as described previously [21]. Antibody controls included omission of the primary antibody or detection of endogenous IgG staining with goat anti-mouse or anti-rabbit IgG (Calbiochem, San Diego, CA). For statistical analysis of the staining scores, Student's *t*-test was performed (see *Statistical analysis*).

Spheroid and wound healing assays and RNA interference

Confluent monolayers of cells were trypsinized. Low cell binding plates were used to seed the cells in corresponding culture medium containing 20ng/mL of FGF, 20ng/mL of EGF (Sigma) and 10mL/500mL of B27 supplement (BD Biosciences) and cultured at 37oC (5% CO2, 100% humidity) . Multicellular spheroids were designated as random spheroids and used for all experiments that employed larger populations of cells. 293T cells were treated with siRNAs of EZH2 or non-targeting control and grown to confluence on 12-well plastic dishes, wounded by scratching with a sharp pipette tip, and washed with fresh media. Wounds were photographed at 0, 12 and 24h intervals with microscope with a 10x objective. A portion of the cells treated with siRNAs was taken separately for Western blot analysis. The siRNA targeting EZH2 (Cat# S102665166) and All Star negative control (Cat# 1027280) were purchased from Qiagen (Germantown, MD) and siRNAs targeting EZH2 (SASI_Hs02_00337644 and SASI_Hs01_00147882) were from Sigma. Cells were transfected with 100 nM final concentrations of siRNA duplexes using Lipofectamine 2000 (Invitrogen) following the manufacturer’s instructions.

Statistical analysis

All experimental results are expressed as mean values standard errors. Statistical analyses of all studies were performed using unpaired, two-tailed Student’s *t* tests. *P* values of 0.05 were considered significant.

Supplementary Material

Refer to Web version on PubMed Central for supplementary material.

Acknowledgments

Grant Support- This work was partially supported by the National Institutes of Health Grant R01 CA131413 and start-up funds from the University of Kansas Medical Center, Kansas City, KS, USA.

Abbreviations

AOM	Azoxymethane
DSS	Dextran Sodium Sulfate
DZnep	3-Deazaneplanocin A
EMT	Epithelial Mesenchymal Transition
PCR2	Polycomb Repressive Complex 2
SAHA	Suberoylanilide Hydroxamic Acid

References

1. Ahmed I, Chandrakesan P, Tawfik O, Xia L, Anant S, Umar S. Critical roles of Notch and Wnt/beta-catenin pathways in the regulation of hyperplasia and/or colitis in response to bacterial infection. Infection and immunity. 2012; 80:3107–3121. [PubMed: 22710872]
2. Ahmed I, Roy B, Chandrakesan P, Venugopal A, Xia L, Jensen R, et al. Evidence of functional cross talk between the Notch and NF-kappaB pathways in nonneoplastic hyperproliferating colonic epithelium. American journal of physiology Gastrointestinal and liver physiology. 2013; 304:G356–370. [PubMed: 23203159]
3. Bachmann IM, Halvorsen OJ, Collett K, Stefansson IM, Straume O, Haukaas SA, et al. EZH2 expression is associated with high proliferation rate and aggressive tumor subgroups in cutaneous melanoma and cancers of the endometrium, prostate, and breast. Journal of clinical oncology : official journal of the American Society of Clinical Oncology. 2006; 24:268–273. [PubMed: 16330673]
4. Boffa LC, Vidali G, Mann RS, Allfrey VG. Suppression of histone deacetylation in vivo and in vitro by sodium butyrate. The Journal of biological chemistry. 1978; 253:3364–3366. [PubMed: 649576]
5. Cao Q, Yu J, Dhanasekaran SM, Kim JH, Mani RS, Tomlins SA, et al. Repression of E-cadherin by the polycomb group protein EZH2 in cancer. Oncogene. 2008; 27:7274–7284. [PubMed: 18806826]
6. Cao Q, Mani RS, Ateeq B, Dhanasekaran SM, Asangani IA, Prensner JR, et al. Coordinated regulation of polycomb group complexes through microRNAs in cancer. Cancer cell. 2011; 20:187–199. [PubMed: 21840484]
7. Chan DW, Chan CY, Yam JW, Ching YP, Ng IO. Prickle-1 negatively regulates Wnt/beta-catenin pathway by promoting Dishevelled ubiquitination/degradation in liver cancer. Gastroenterology. 2006; 131:1218–1227. [PubMed: 17030191]
8. Chandrakesan P, Ahmed I, Anwar T, Wang Y, Sarkar S, Singh P, et al. Novel changes in NF-{kappa}B activity during progression and regression phases of hyperplasia: role of MEK, ERK, and p38. The Journal of biological chemistry. 2010; 285:33485–33498. [PubMed: 20710027]
9. Chandrakesan P, Jakkula LU, Ahmed I, Roy B, Anant S, Umar S. Differential Effects of beta-catenin and NF-kappaB Interplay in the Regulation of Cell Proliferation, Inflammation and Tumorigenesis in Response to Bacterial Infection. PloS one. 2013; 8:e79432. [PubMed: 24278135]

10. Chandrakesan P, Roy B, Jakkula LU, Ahmed I, Ramamoorthy P, Tawfik O, et al. Utility of a bacterial infection model to study epithelial-mesenchymal transition, mesenchymal-epithelial transition or tumorigenesis. Oncogene. 2013
11. Cheng AS, Lau SS, Chen Y, Kondo Y, Li MS, Feng H, et al. EZH2-mediated concordant repression of Wnt antagonists promotes beta-catenin-dependent hepatocarcinogenesis. Cancer research. 2011; 71:4028–4039. [PubMed: 21512140]
12. Clevers H, Nusse R. Wnt/beta-catenin signaling and disease. Cell. 2012; 149:1192–1205. [PubMed: 22682243]
13. Deng W, Puente JL, Gruenheid S, Li Y, Vallance BA, Vazquez A, et al. Dissecting virulence: systematic and functional analyses of a pathogenicity island. Proceedings of the National Academy of Sciences of the United States of America. 2004; 101:3597–3602. [PubMed: 14988506]
14. Hamon MA, Cossart P. Histone modifications and chromatin remodeling during bacterial infections. Cell host & microbe. 2008; 4:100–109. [PubMed: 18692770]
15. Hayashi Y, Tsujii M, Wang J, Kondo J, Akasaka T, Jin Y, et al. CagA mediates epigenetic regulation to attenuate let-7 expression in Helicobacter pylori-related carcinogenesis. Gut. 2013; 62:1536–1546. [PubMed: 22936674]
16. Ihara A, Wada K, Yoneda M, Fujisawa N, Takahashi H, Nakajima A. Blockade of leukotriene B4 signaling pathway induces apoptosis and suppresses cell proliferation in colon cancer. Journal of pharmacological sciences. 2007; 103:24–32. [PubMed: 17220595]
17. Joshi P, Carrington EA, Wang L, Ketel CS, Miller EL, Jones RS, et al. Dominant alleles identify SET domain residues required for histone methyltransferase of Polycomb repressive complex 2. The Journal of biological chemistry. 2008; 283:27757–27766. [PubMed: 18693240]
18. Jung HY, Jun S, Lee M, Kim HC, Wang X, Ji H, et al. PAF and EZH2 induce Wnt/beta-catenin signaling hyperactivation. Molecular cell. 2013; 52:193–205. [PubMed: 24055345]
19. Kleer CG, Cao Q, Varambally S, Shen R, Ota I, Tomlins SA, et al. EZH2 is a marker of aggressive breast cancer and promotes neoplastic transformation of breast epithelial cells. Proceedings of the National Academy of Sciences of the United States of America. 2003; 100:11606–11611. [PubMed: 14500907]
20. Kondo Y, Shen L, Cheng AS, Ahmed S, Boumber Y, Charo C, et al. Gene silencing in cancer by histone H3 lysine 27 trimethylation independent of promoter DNA methylation. Nature genetics. 2008; 40:741–750. [PubMed: 18488029]
21. Li X, Gonzalez ME, Toy K, Filzen T, Merajver SD, Kleer CG. Targeted overexpression of EZH2 in the mammary gland disrupts ductal morphogenesis and causes epithelial hyperplasia. The American journal of pathology. 2009; 175:1246–1254. [PubMed: 19661437]
22. Lombaerts M, van Wezel T, Philippo K, Dierssen JW, Zimmerman RM, Oosting J, et al. E-cadherin transcriptional downregulation by promoter methylation but not mutation is related to epithelial-to-mesenchymal transition in breast cancer cell lines. British journal of cancer. 2006; 94:661–671. [PubMed: 16495925]
23. Lu J, He ML, Wang L, Chen Y, Liu X, Dong Q, et al. MiR-26a inhibits cell growth and tumorigenesis of nasopharyngeal carcinoma through repression of EZH2. Cancer research. 2011; 71:225–233. [PubMed: 21199804]
24. Miranda TB, Cortez CC, Yoo CB, Liang G, Abe M, Kelly TK, et al. DZNep is a global histone methylation inhibitor that reactivates developmental genes not silenced by DNA methylation. Molecular cancer therapeutics. 2009; 8:1579–1588. [PubMed: 19509260]
25. Newman JV, Kosaka T, Sheppard BJ, Fox JG, Schauer DB. Bacterial infection promotes colon tumorigenesis in Apc(Min/+) mice. The Journal of infectious diseases. 2001; 184:227–230. [PubMed: 11424022]
26. Sasaki M, Ikeda H, Itatsu K, Yamaguchi J, Sawada S, Minato H, et al. The overexpression of polycomb group proteins Bmi1 and EZH2 is associated with the progression and aggressive biological behavior of hepatocellular carcinoma. Laboratory investigation; a journal of technical methods and pathology. 2008; 88:873–882.
27. Sauvageau M, Sauvageau G. Polycomb group proteins: multi-faceted regulators of somatic stem cells and cancer. Cell stem cell. 2010; 7:299–313. [PubMed: 20804967]

28. Sellin JH, Umar S, Xiao J, Morris AP. Increased beta-catenin expression and nuclear translocation accompany cellular hyperproliferation in vivo. Cancer research. 2001; 61:2899–2906. [PubMed: 11306465]

29. Sellin JH, Wang Y, Singh P, Umar S. beta-Catenin stabilization imparts crypt progenitor phenotype to hyperproliferating colonic epithelia. Experimental cell research. 2009; 315:97–109. [PubMed: 18996369]

30. Shen L, Cui J, Liang S, Pang Y, Liu P. Update of research on the role of EZH2 in cancer progression. OncoTargets and therapy. 2013; 6:321–324. [PubMed: 23589697]

31. Taniguchi H, Jacinto FV, Villanueva A, Fernandez AF, Yamamoto H, Carmona FJ, et al. Silencing of Kruppel-like factor 2 by the histone methyltransferase EZH2 in human cancer. Oncogene. 2012; 31:1988–1994. [PubMed: 21892211]

32. Umar S, Morris AP, Kourouma F, Sellin JH. Dietary pectin and calcium inhibit colonic proliferation in vivo by differing mechanisms. Cell proliferation. 2003; 36:361–375. [PubMed: 14710853]

33. Umar S, Wang Y, Sellin JH. Epithelial proliferation induces novel changes in APC expression. Oncogene. 2005; 24:6709–6718. [PubMed: 16007167]

34. Umar S, Wang Y, Morris AP, Sellin JH. Dual alterations in casein kinase I-epsilon and GSK-3beta modulate beta-catenin stability in hyperproliferating colonic epithelia. American journal of physiology Gastrointestinal and liver physiology. 2007; 292:G599–607. [PubMed: 17053159]

35. Umar S. Citrobacter Infection and Wnt signaling. Current colorectal cancer reports. 2012; 8

36. Wellner U, Schubert J, Burk UC, Schmalhofer O, Zhu F, Sonntag A, et al. The EMT-activator ZEB1 promotes tumorigenicity by repressing stemness-inhibiting microRNAs. Nature cell biology. 2009; 11:1487–1495. [PubMed: 19935649]

37. Wissmann C, Wild PJ, Kaiser S, Roepcke S, Stoehr R, Woenckhaus M, et al. WIF1, a component of the Wnt pathway, is down-regulated in prostate, breast, lung, and bladder cancer. The Journal of pathology. 2003; 201:204–212. [PubMed: 14517837]

38. Zhang X, Zhao X, Fiskus W, Lin J, Lwin T, Rao R, et al. Coordinated silencing of MYC-mediated miR-29 by HDAC3 and EZH2 as a therapeutic target of histone modification in aggressive B-Cell lymphomas. Cancer cell. 2012; 22:506–523. [PubMed: 23079660]

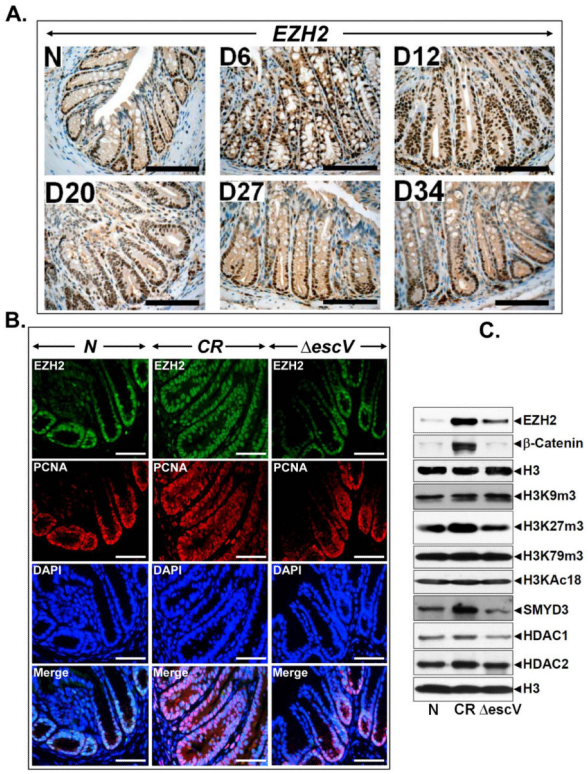

Figure 1. Effect of CR infection on EZH2 expression and colocalization with proliferation marker

A. Paraffin-embedded sections prepared from the distal colons of uninfected normal (N) or days 6-34 post-CR-infected mice (D6-D34) were stained with EZH2 antibody. Percentages represent percent cells positive for EZH2. Scale bar = 75 μm (n = 3 independent experiments). **B.** Paraffin-embedded sections prepared from uninfected normal (N) and either wild type CR or ΔescV mutant-infected mouse distal colons were co-stained with antibodies for EZH2 and PCNA (a marker of proliferation). DAPI was used to label nuclei. Scale bar = 100 μm (n = 3 independent experiments). **C.** Nuclear protein extracts prepared from the colonic crypts of mice described in **B** were subjected to Western blotting with antibodies specific to indicated proteins.

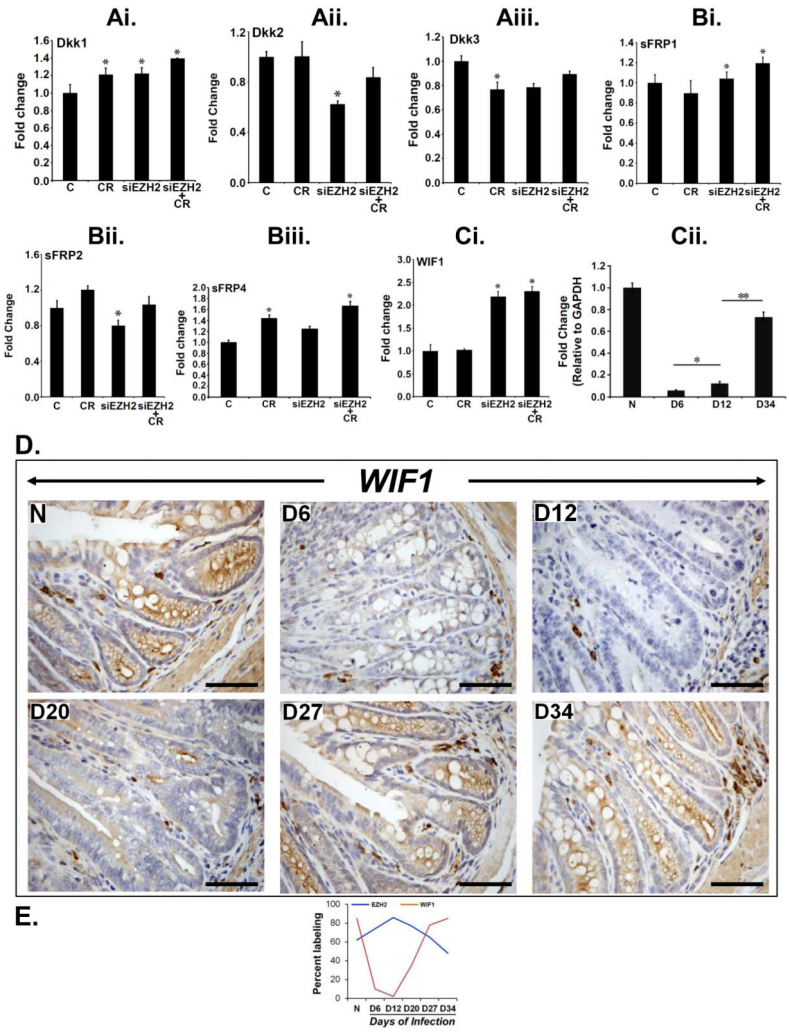

Figure 2. EZH2 downregulation promotes expression of Wnt antagonists

Ai-Ci. Uninfected control (C) or CR infected HEK-293T cells were transfected with specific siRNA to EZH2 and total RNA isolated from these cells were subjected to real-time RT-PCR with primers specific for various Wnt antagonists as indicated. Relative gene expression in terms of fold change is shown (*$p<0.05$; n = 5 independent experiments). **Cii.** Real-time PCR for WIF1 expression in the colonic crypts of uninfected normal or days 6, 12 and 34 post-CR infected mice (*, ** $p<0.05$; n = 3 independent experiments). **D.** Paraffin-embedded sections prepared from the distal colons of uninfected normal (N) or days6-34 post-CR-infected mice (D6-D34) were stained with antibody specific for WIF1. Scale bar = 100 μm (n = 3 independent experiments). **E.** Line plot showing reciprocal relationship between EZH2 and WIF1 (n = 3 independent experiments).

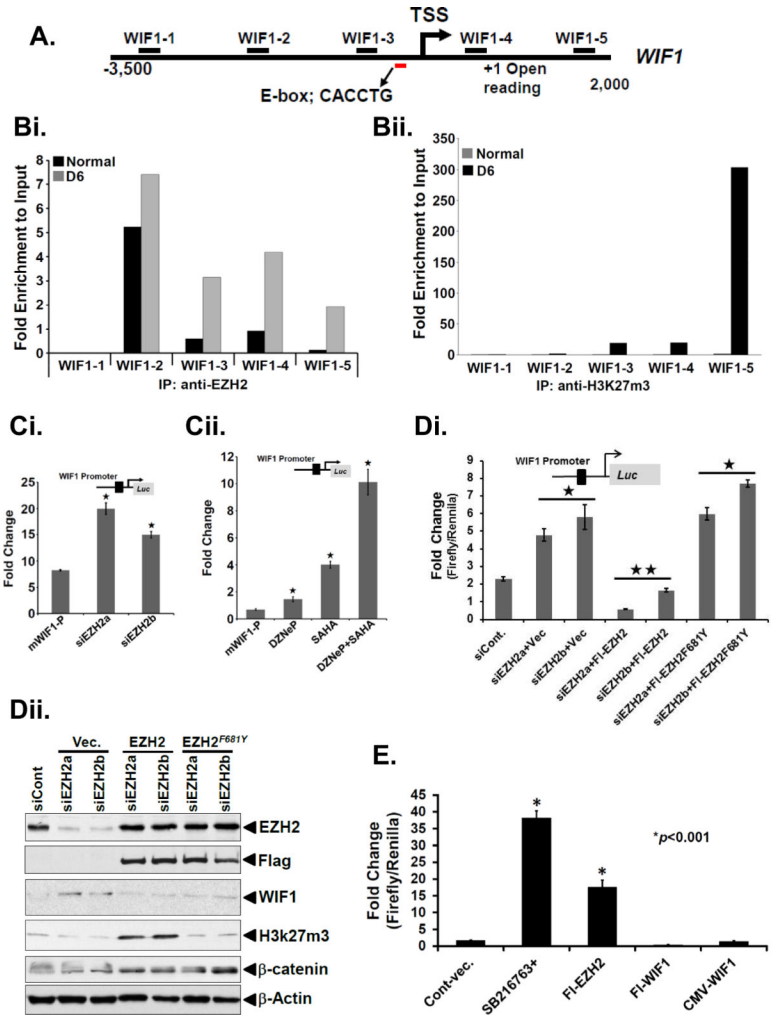

Figure 3. EZH2 targets WIF1 promoter

A. Regions of mouse WIF1 promoter located on chromosome 10, were analyzed via Chromatin immunoprecipitation (ChIP)-PCR assay as described below. **B. ChIP-PCR assay.** Crypt cells were isolated from uninfected normal or day-6 post-infected distal colons. A ChIP assay was performed with antibodies specific to EZH2 (**Bi**) and H3K27me3 (**Bii**), respectively. The DNA purified after ChIP was evaluated by semi quantitative PCR using primers specific for regions of WIF1 promoter described in **A**. The bar graphs represent the fold enrichment relative to input (n = 3 independent experiments). C. Effect of EZH2 knockdown on WIF1 promoter activity. HEK-293T cells were transfected with WIF1-Luc reporter vector for 24 hours followed by depletion of EZH2 with either specific siRNAs (**Ci**) or treatment with DZNep and SAHA either alone or in combination for another 24 hours (**Cii**) followed by measurement of reporter activity (*p<0.05; n = 5 independent experiments). Di-Dii. Methyltransferase function is required for WIF1 regulation. Di. Measurement of WIF1 promoter activity following EZH2 knockdown or overexpression of either wild type or F681Y mutant (* and **p<0.05; n = 3 independent experiments). **Dii.** Group of cells described in **Di** were Western blotted for indicated proteins (n = 3 independent experiments). **E. WIF1 regulates Wnt signaling**. 293-HEK cells transfected

with TOPflash reporter were either treated with GSK-3β inhibitor for 24 h or transiently co-transfected with EZH2 or WIF1 cDNAs followed by measurement of reporter activity (*P<0.001 vs. control; n = 3 independent experiments).

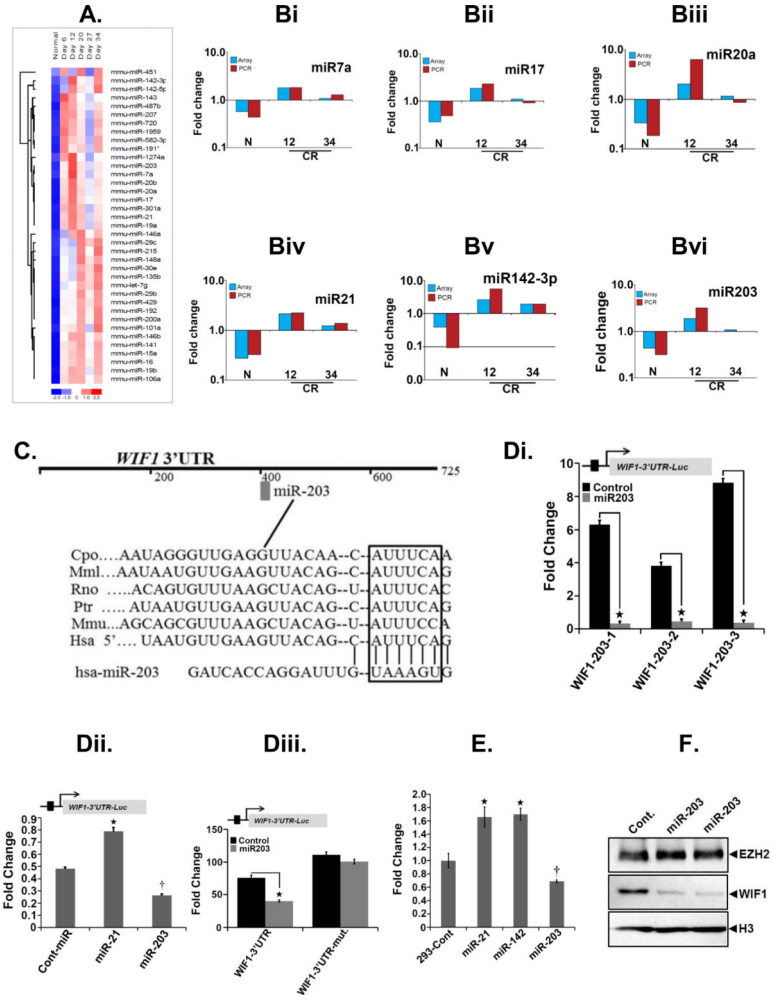

Figure 4. Effect of CR infection on miRNA expression *in vivo*

A. Total RNA extracted from the distal colonic crypts of uninfected normal or days6-34 post-CR-infected mice (Day 6-Day 34) was subjected to a miRNA array. A representative heat map showing the average expression intensities of indicated miRNAs. **B. Validation of array data**. Indicated miRNAs (**Bi-Bvi**) were amplified via real-time PCR and expression kinetics was compared with the respective array profile (N, uninfected control; 12 and 34, days-12 and 34 post-CR infection). **C.** Highly conserved, predicted binding sites for the seed sequences of miR-203 in the 3'UTR of *WIF1* mRNA. Di-Diii. Effect of miR-203 overexpression on WIF promoter activity. HEK-293T cells were either transiently (**Di**) or stably (**Dii**) transfected with miR-203 (**Di, Dii**) as well as miR-21 (**Dii**) mimics followed by measurement of *WIF1* 3'UTR-luciferase activity (*p<0.05; n = 5 independent experiments). **Diii.** Measurement of *WIF1* 3'UTR-luciferase activity in cells transfected with pGL4-Luc vector containing either wild type or mutated miR-203 binding site in *WIF1* 3'UTR (*p<0.05; n = 5 independent experiments). E. Effect of miRNA overexpression on WIF1 transcription. HEK-293T cells were transfected with indicated miRNA mimics followed by measurement of WIF1 expression by real-time RT-PCR (*, †p<0.05; n = 5 independent experiments). **F. Effect of miRNA overexpression on WIF1**. HEK-293T cells were

transfected with indicated miRNA mimics followed by measurement of WIF1 protein levels by Western blotting. H3 is the loading control.

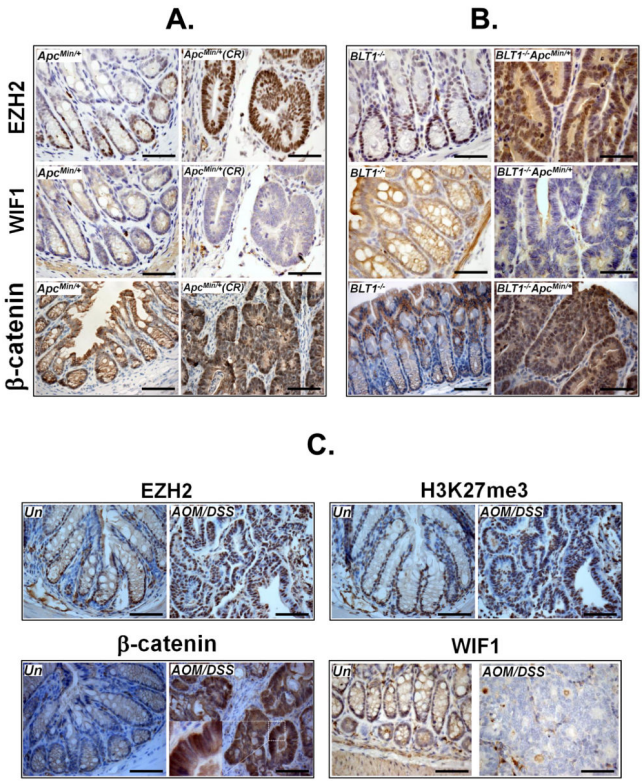

Figure 5. Validation of EZH2 and WIF1 inverse expression profile in various models of colon cancer

Representative photomicrographs of paraffin embedded sections prepared from the distal colons of: **A,** Uninfected normal (*Apc*$^{Min/+}$) or CR-infected *Apc*$^{Min/+}$ mice [*Apc*$^{Min/+}$(CR)] at 3 months of age; **B,** *BLT1*$^{-/-}$ mice or *Apc*$^{Min/+}$ mice at 110 days; **C.** Untreated or AOM +DSS-treated ICR mice at 168 days. Sections were stained with antibodies for: EZH2, β-catenin, WIF1 and H3K27me3, respectively (Bar = 50μm; n = 3 independent experiments).

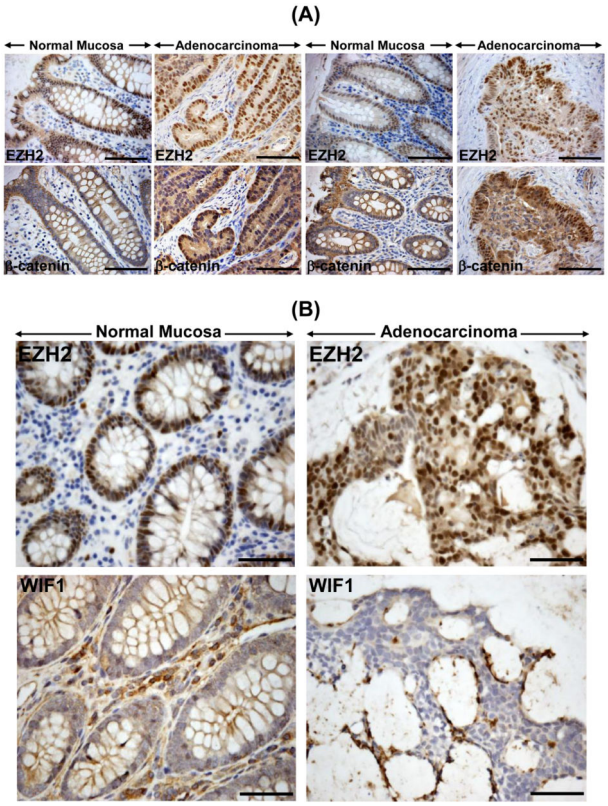

Figure 6. Relevance of changes in EZH2, β-catenin and WIF1 expression to humans

Representative photomicrographs of paraffin embedded sections prepared from humans with adenocarcinoma and either without (**A**, left panel) or with (**A**, right panel; **B**, lower panel) invasive front. Sections were stained with antibodies for: EZH2, β-catenin and WIF1 (Original magnification = 200X; n = 2 independent experiments). A total of 18 de-identified adenoma/adenocarcinoma samples and the corresponding controls were analyzed for EZH2 and WIF1 staining. Significant inverse correlation between EZH2 and WIF1 labeling were recorded that paralleled staining pattern observed with mouse models of colon cancer.